The role of dissolved molecular oxygen in abiotic pyrite oxidation under acid pH conditions – Experiments with 18O-enriched molecular oxygen

ARTICLE *in* APPLIED GEOCHEMISTRY · NOVEMBER 2010

Impact Factor: 2.27 · DOI: 10.1016/j.apgeochem.2010.08.014

2 AUTHORS:

Claudia Heidel
Technische Universität Bergakademie Frei…
9 PUBLICATIONS **99** CITATIONS
SEE PROFILE

M. Tichomirowa
Technische Universität Bergakademie Frei…
59 PUBLICATIONS **855** CITATIONS
SEE PROFILE

Applied Geochemistry 25 (2010) 1664–1675

Contents lists available at ScienceDirect

Applied Geochemistry

journal homepage: www.elsevier.com/locate/apgeochem

The role of dissolved molecular oxygen in abiotic pyrite oxidation under acid pH conditions – Experiments with ^{18}O-enriched molecular oxygen

Claudia Heidel *, Marion Tichomirowa

Institute of Mineralogy, TU Bergakademie Freiberg, Brennhausgasse 14, 09599 Freiberg, Germany

ARTICLE INFO

Article history:
Received 18 December 2009
Accepted 25 August 2010
Available online 20 September 2010
Editorial handling by R. R. Seal

ABSTRACT

Several O isotope studies have shown that SO_4^{2-} produced from aqueous pyrite oxidation mainly contains water-derived O and minor atmospherically-derived O_2. However, the incorporation of O_2 into SO_4^{2-} has been shown to decrease continuously during pyrite oxidation experiments. Hence, it remains uncertain if (and how) O_2 is permanently incorporated into SO_4^{2-} during pyrite oxidation.

Abiotic aerobic batch pyrite oxidation experiments in aqueous solutions were performed under acid pH conditions. After 151 days, ^{18}O-enriched O_2 was injected into the headspace of the reaction vessels. Increasing $\delta^{18}O_{SO_4}$ values with increasing injection volume of ^{18}O-enriched O_2 indicated the permanent incorporation of about 9% O_2 into the produced SO_4^{2-} during pyrite oxidation from 151 to 201 days. Molecular oxygen may be incorporated into SO_4^{2-} by oxidation of the S intermediate species sulfite (and maybe tetrathionate) into SO_4^{2-}. However, only 4% of the O_2 consumed during the experiments was incorporated into SO_4^{2-}. Slightly increased $\delta^{18}O_{H_2O}$ values from experiments with the largest injection of ^{18}O-enriched O_2 indicated the incorporation of O_2 into water molecules which may proceed during the cathodic reduction of O_2. Thus, O_2 was an important electron acceptor under aerobic acid conditions. The observed $\varepsilon_{SO_4-O_2}$ value indicated that the oxidation of dissolved Fe^{2+} by O_2 did not play an important role. Furthermore, the lack of ^{32}S enrichment in SO_4^{2-} compared to pyrite indicated that the oxidation of adsorbed Fe^{2+} by O_2 should not be a dominant mechanism, although it may be catalyzed onto the pyrite surface. Hence, O_2 should accept electrons predominantly from pyrite.

1. Introduction

Pyrite oxidation produces acid waters with high SO_4^{2-}, Fe and trace metal contents (Acid Mine Drainage – AMD). It can be described by two reactions with either O_2 or Fe^{3+} as oxidant, i.e., electron acceptor (Singer and Stumm, 1970):

$$FeS_2 + 3.5O_2 + H_2O \rightarrow Fe^{2+} + 2SO_4^{2-} + 2H^+ \quad (1)$$

$$FeS_2 + 14Fe^{3+} + 8H_2O \rightarrow 15Fe^{2+} + 2SO_4^{2-} + 16H^+. \quad (2)$$

Under acid pH conditions, reaction (2) is rate-limited by the oxidation of Fe^{2+} to Fe^{3+} (Singer and Stumm, 1970):

$$Fe^{2+} + 0.25O_2 + H^+ \rightarrow Fe^{3+} + 0.5H_2O. \quad (3)$$

Reactions (1) and (2) are simplifications of the general oxidation mechanism. The oxidation of pyrite (S^-) to SO_4^{2-} requires the transfer of seven electrons per mole of S. Because only one or two electrons can be transferred in one step (Basolo and Pearson, 1967), intermediate S species with oxidation states between −1 and +6 should be formed. However, single oxidation steps (including electron acceptors and O sources) and the location of the reactions (on pyrite surface or in solution) are still under discussion.

Knowledge of pyrite oxidation mechanisms is prerequisite to interpret and evaluate data from natural sites as recently discussed by Hubbard et al. (2009). Oxygen (and S isotopes) of dissolved SO_4^{2-} may help to evaluate the role and relative importance of O_2 in pyrite oxidation mechanisms (Seal, 2003). According to reactions (1) and (2), O in the produced SO_4^{2-} can originate from atmospheric-derived dissolved O_2 and water. The relative proportion of O in SO_4^{2-} from the two potential sources can be calculated by means of the following equation from Lloyd (1967) which was later named "general isotope-balance model" (Taylor and Wheeler, 1994):

$$\delta^{18}O_{SO_4} = X(\delta^{18}O_{H_2O} + \varepsilon_{SO_4-H_2O}) + (1-X)(\delta^{18}O_{O_2} + \varepsilon_{SO_4-O_2}). \quad (4)$$

$\delta^{18}O_{SO_4}$, $\delta^{18}O_{H_2O}$, and $\delta^{18}O_{O_2}$ are the O isotope compositions of SO_4^{2-}, water ($\delta^{18}O_{H_2O} < 0$ for meteoric waters), and O_2 ($\delta^{18}O_{O_2} = 23.5‰$, Kroopnick and Craig, 1972), respectively. X is the proportion of O in SO_4^{2-} derived from water, $(1-X)$ is the resulting proportion of O in SO_4^{2-} derived from O_2, $\varepsilon_{SO_4-H_2O}$ is the O isotope enrichment factor between SO_4^{2-} and water and $\varepsilon_{SO_4-O_2}$ is the O isotope enrichment factor between SO_4^{2-} and O_2.

Published $\varepsilon_{SO_4-H_2O}$ values range from 0.0‰ to 4.0‰ for abiotic acid conditions (Taylor et al., 1984: 4.0‰, Taylor and Wheeler,

* Corresponding author. Tel.: +49 3731 392656; fax: +49 3731 394060.
E-mail address: claudia.heidel@gmx.net (C. Heidel).

0883-2927/$ - see front matter © 2010 Elsevier Ltd. All rights reserved.
doi:10.1016/j.apgeochem.2010.08.014

1994: 0.0‰, Balci et al., 2007: 2.9‰, Mazumdar et al., 2008: 2.6‰). Values for $\varepsilon_{SO_4-O_2}$ of −4.3‰ (Taylor et al., 1984) and −9.8‰ (Balci et al., 2007) were determined from abiotic pyrite oxidation experiments. Depending on the $\varepsilon_{SO_4-H_2O}$ and $\varepsilon_{SO_4-O_2}$ values used, calculations of the relative proportions of O in SO_4^{2-} from both sources (X and $(1-X)$) by means of the general isotope-balance model bear an uncertainty of ±10% (Toran, 1986). Nevertheless, O isotope studies of aerobic abiotic pyrite oxidation under acid pH conditions have indicated that most of the O in the produced SO_4^{2-} originated from water (at the end of the experiments); but a small amount of O in SO_4^{2-} derived from O_2 (Taylor et al., 1984; Reedy et al., 1991; Balci et al., 2007; Tichomirowa and Junghans, 2009; Heidel et al., 2009).

Abiotic and biotic pyrite oxidation studies have shown that $\delta^{18}O_{SO_4}$ values changed with time and became more similar to the $\delta^{18}O$ value of the water (Taylor et al., 1984; Gould et al., 1989; Reedy et al., 1991; Balci et al., 2007; Pisapia et al., 2007; Heidel et al., 2009; Tichomirowa and Junghans, 2009). Thus, the relative proportion of water-derived O and O_2 in SO_4^{2-} changed during pyrite oxidation experiments. Tichomirowa and Junghans (2009) varied the experiment duration from 2 to 100 days. They calculated from their $\delta^{18}O_{SO_4}$ values that 32–69% O_2 was incorporated into the initially produced SO_4^{2-}. After 100 days, decreased $\delta^{18}O_{SO_4}$ values indicated a proportion of 2–24% O_2 in SO_4^{2-} (Tichomirowa and Junghans, 2009). Heidel et al. (2009) extended the experiment duration to 300 days and observed that constant $\delta^{18}O_{SO_4}$ values were already achieved after 100 days of experiments which started at pH 6 but rapidly decreased to acid pH (⩽3 after 50 days). In contrast, $\delta^{18}O_{SO_4}$ values seemed to decrease slightly even from 100 to 200 days in experiments at an initial pH 2 (Heidel et al., 2009) which may be attributed to a slower oxidation rate due to the pH conditions and due to the use of a larger pyrite grain size.

Heidel et al. (2009) observed that the final constant difference between $\delta^{18}O_{SO_4}$ and $\delta^{18}O_{H_2O}$ values varied between 3.3‰ and 4.0‰ which was in the range of published $\varepsilon_{SO_4-H_2O}$ values (0.0–4.0‰). However, it remained uncertain if the final difference between $\delta^{18}O_{SO_4}$ and $\delta^{18}O_{H_2O}$ values equaled the $\varepsilon_{SO_4-H_2O}$ value (i.e., if the relative proportion of O_2 in SO_4^{2-} decreased to 0%) or if it exceeded the $\varepsilon_{SO_4-H_2O}$ value (i.e., if a small proportion of O_2 was permanently incorporated into SO_4^{2-} throughout the experiments).

This study should show if O_2 is only initially or permanently (i.e., also at later stages of oxidation) incorporated into the produced SO_4^{2-} during abiotic pyrite oxidation. Experiments started at pH 2.3 which was somewhat higher than the initial pH 2 from Heidel et al. (2009). Furthermore, the smaller grain size used in the present experiments (63–100 μm) also resulted in a faster pyrite oxidation compared with experiments with the 100–140 μm and 140–180 μm from Heidel et al. (2009). Therefore, constant $\delta^{18}O_{SO_4}$ values and, thus, constant relative proportions of water-derived and O_2 should be achieved after 151 days of oxidation. Then, ^{18}O-enriched O_2 was injected into the headspace of the reaction vessels and pyrite was allowed to keep oxidizing until experiments were finished after 201 days. The incorporation of ^{18}O-enriched O_2 into SO_4^{2-} should be reflected in the O isotope composition of the produced SO_4^{2-}. The proportion of O_2 in SO_4^{2-} should be quantified. Results may contribute to the understanding of the role of O_2 in pyrite oxidation mechanisms.

2. Material and methods

2.1. Pyrite

Tichomirowa and Junghans (2009) and Heidel et al. (2009) observed that O_2 was adsorbed particularly on ultrafine pyrite particles and incorporated into the produced SO_4^{2-}. Ground pyrite from Peru was sieved to obtain grain size 63–100 μm to prevent this effect. Before starting the experiments, fine pyrite particles and sulfate coatings on pyrite surfaces were removed by a cleaning procedure similar to that described in Moses et al. (1987). Pyrite grains were put into hot 6 M HCl for about 10 min. Subsequently, the grains were washed with deionized water, rinsed in ethanol, and dried in a desiccator. The $\delta^{34}S$ value of the pre-treated pyrite was 2.5 ± 0.3‰ (1σ, $n = 8$). A specific surface area of 0.059 ± 0.018 (1σ, $n = 6$) $m^2\ g^{-1}$ was determined by BET measurements at the Granulometric Laboratory of the Institute of Electronic and Sensor Materials, TU Bergakademie Freiberg.

2.2. Experiments

Experiments were carried out with two different waters: arctic rainfall ($\delta^{18}O_{H_2O} = -17.5‰$) and ultrapure (18.2 MΩ cm) deionized water ($\delta^{18}O_{H_2O} = -8.9‰$). An initial pH of 2.3 was adjusted by adding 1 M HCl. Prior to the experiments, the water was filter-sterilized by filtration through 0.2 μm cellulose nitrate filters (Macherey–Nagel). Two hundred and fifty mL water and 25 g pyrite were placed in a flask with a volume of about 550 mL. The headspace (ca. 300 mL) was initially filled with ambient air ($p_{O_2} = 0.21$ atm). Experiments were performed in a closed system (i.e., flasks were sealed) to avoid evaporation effects and to enable the determination of $\varepsilon_{SO_4-O_2}$. Pyrite was allowed to oxidize in a dark air-conditioned room at 21 °C for 151 days.

To reduce the extremely high $\delta^{18}O_{O_2} = 24,211,049‰$ of ^{18}O-enriched pure O_2 (97.1 atom% ^{18}O, 2.0 atom% ^{16}O, obtained from Campro Scientific), it was mixed with air ($\delta^{18}O_{O_2} = 23.5‰$, Kroopnick and Craig, 1972). The $\delta^{18}O_{O_2}$ value of the mixture was 19,000‰. Different volumes (250, 500, and 1000 μL) of this gas were injected through a septum into the headspace of the experiment flasks by means of a gastight syringe (Hamilton). Absolute amounts of injected ^{18}O-enriched O_2 were 0.0022 mmol (for 250 μL), 0.0044 mmol (for 500 μL), and 0.0087 mmol (for 1000 μL). After the injection of ^{18}O-enriched O_2, pyrite was allowed to continue oxidizing until the experiments were finished after 201 days. Simultaneously, two control experiments were performed without injection of ^{18}O-enriched O_2.

2.3. Morphological and mineralogical investigations

After finishing the experiments, pyrite was dried in a desiccator. The pyrite grain morphology was observed by scanning electron microscopy (SEM) (JSM-6400 from JEOL) and the composition was determined by energy-dispersive X-ray analysis (EDX) (Noran Vantage from Noran Instruments) at the SEM laboratory of the Institute of Geology, TU Bergakademie Freiberg.

2.4. Hydrochemical measurements

Dissolved O_2 (DO) concentrations were measured non-invasively from outside through the wall of the flasks several times during the experiments by an oxygen meter connected to fiber-optic oxygen minisensors which were glued inside the vessels (Fibox 3 with planar oxygen-sensitive spots from PreSens). The instrument's detection limit is 0.0005 mmol L^{-1} DO. An uncertainty of ±1% at 100% air-saturation and ±0.15% at 1% air-saturation is given by the instrument's manufacturer. Hence, the uncertainty should be better than ±1% during the DO measurements.

At the end of the experiments, pH values were measured by means of a pH electrode (pH 340 with a SenTix 41 sensor from WTW). Ferrous and total Fe concentrations were immediately determined spectrophotometrically using the 1,10 phenanthroline method (photoLab S12 from WTW). Aliquots for the determination of SO_4^{2-} were stored in a refrigerator and analyzed within one

week. Formaldehyde was added to aliquots for sulfite and thiosulfate determination before they were also stored in a refrigerator. Sulfate, sulfite, and thiosulfate concentrations were measured by ion chromatography (DX-120 from Dionex) at the Geochemical–Analytical Laboratory of the Institute of Mineralogy, TU Bergakademie Freiberg. Relative errors (1σ) were better than 10% for Fe and 7% for sulfate, sulfite, and thiosulfate based on repeated measurements of standards.

2.5. Isotope measurements

Oxygen isotopes of O_2, water and SO_4^{2-}, and S isotopes of SO_4^{2-} and pyrite were measured on a mass spectrometer Delta plus (Finnigan MAT) at the Geochemical Isotope Laboratory of the Institute of Mineralogy, Freiberg. The common δ-notation is used for reporting isotope ratios:

$$\delta = \left[\left(\frac{R_{sample}}{R_{standard}}\right) - 1\right] \times 1000(‰), \quad (5)$$

where $R = {}^{18}O/{}^{16}O$ and $R = {}^{34}S/{}^{32}S$, relative to the standard Vienna-Standard Mean Ocean Water (V-SMOW) for $\delta^{18}O$ and Vienna-Canyon Diablo Troilite (V-CDT) for $\delta^{34}S$.

$\delta^{18}O_{O_2}$ values of dissolved O_2 were measured as $\delta^{18}O_{O_2}$ values of the headspace gas (Oba and Poulson, 2009a). The measuring technique was modified after Wassenaar and Koehler (1999). An aliquot of the headspace gas flowed into an evacuated capillary and got through a sample loop into a He flow. Oxygen was separated from other gases by carrying the sample through a water and CO_2 trap and a gas chromatography column before entering the mass spectrometer. Isotope analyses were compared against air ($\delta^{18}O_{O_2} = 23.5‰$, Kroopnick and Craig, 1972).

$\delta^{18}O_{H_2O}$ values were measured by isotope ratio mass spectrometry with a dual inlet system after equilibrating the water with CO_2 (Epstein and Mayeda, 1953).

Sulfate for O and S isotope measurements was prepared as follows: the pH of the aqueous solution was adjusted to >7 with 1 M NaOH to precipitate Fe. After filtration, the pH was adjusted to about 3.5 with 1 M HCl and $BaSO_4$ was precipitated by adding $BaCl_2$ into the heated solution. Afterwards, precipitated $BaSO_4$ was collected on a 0.45 μm cellulose nitrate filter (Sartorius) and rinsed with deionized water to remove Cl^-. $\delta^{18}O_{SO_4}$ values and $\delta^{34}S_{SO_4}$ values were measured by continuous flow isotope ratio mass spectrometry (CF-IRMS) using pyrolysis (e.g., Kornexl et al., 1999) and an elemental analyzer EA 1110 from Carlo Erba (e.g., Giesemann et al., 1994), respectively. Oxygen isotope ratios were normalized to NBS 127, IAEA-SO-5, and IAEA-SO-6 ($\delta^{18}O = 8.7‰$, $\delta^{18}O = 12.0‰$, and $\delta^{18}O = -11.0‰$, Kornexl et al., 1999) and S isotope ratios were normalized to an internal silver sulfide standard and IAEA-SO-2 and IAEA-SO-3 ($\delta^{34}S = 22.7‰$ and $\delta^{34}S = -32.3‰$; Ding et al., 2001). All samples were measured at least in triplicate.

Reproducibility (1σ) was better than 0.2‰ for $\delta^{18}O_{H_2O}$, 0.5‰ for $\delta^{18}O_{O_2}$ and $\delta^{18}O_{SO_4}$, and 0.3‰ for $\delta^{34}S_{SO_4}$ and $\delta^{34}S_{pyrite}$.

3. Results

3.1. SEM investigations

SEM photographs (Fig. 1) showed that there were a few ultrafine particles in the 63–100 μm pyrite fraction which are attributed to the absence of an ultrasonic bath during the pretreatment procedure. However, most of the fine particles were removed by washing the pyrite in HCl and deionized water.

SEM photographs showed that some pits occurred on the pyrite surface; but a lot of particles with clean surfaces without any visual corrosion pits were also present. There were no obvious differences between pyrite from control experiments without injection of ^{18}O-enriched O_2 and pyrite from experiments with the greatest ^{18}O-enriched O_2 injection of 1000 μL (Fig. 1).

No S- and O-containing precipitates could be detected on the pyrite surfaces by EDX analyses.

3.2. Hydrochemistry

Dissolved O_2 concentrations (0.2334 mmol L^{-1} at the beginning) decreased to 0.0463–0.0656 mmol L^{-1} after 201 days (Table 1) and were independent of the ^{18}O-enriched O_2 volume which was injected after 151 days. Based on the measured DO concentrations, absolute amounts of O_2 in the aqueous and gaseous phase were calculated by means of Henry's law and the Ideal gas law (Table 1). The initial total amount of O_2 in the whole system (dissolved and in headspace gas) was 2.270 mmol and decreased to 0.450–0.637 mmol O_2 after 201 days, i.e., 1.632–1.820 mmol O_2 was consumed during the experiments (Table 1, Fig. 2).

Decreasing pH and increasing SO_4^{2-} and Fe concentrations showed the formation of the expected oxidation products according to reactions (1) and (2) (Table 2). Pyrite oxidation rates were estimated based on the amount of the produced SO_4^{2-} (Gleisner et al., 2006):

$$R_{FeS_2} = \frac{a}{A_{BET} \cdot m \cdot c} (\text{mol m}^{-2}\ \text{s}^{-1}), \quad (6)$$

where R_{FeS_2} is the pyrite oxidation rate, a is the slope (mol s^{-1}) from the linear regression of SO_4^{2-} concentration vs. time, A_{BET} is the specific surface area of the pyrite grain size fraction ($m^2\ g^{-1}$), m is the pyrite mass (g), and c is a stoichiometric factor which is 2 for S (and 1 for Fe if the oxidation rate is based on Fe concentrations). Oxidation rates were based on initial SO_4^{2-} concentrations (0 mmol L^{-1}) and concentrations measured after 201 days. Calculated oxidation rates ($9.0 \pm 0.3 \times 10^{-11}$ (1σ, $n = 8$) mol m^{-2} s^{-1}) from experiments with different volumes of injected ^{18}O-enriched O_2 were similar be-

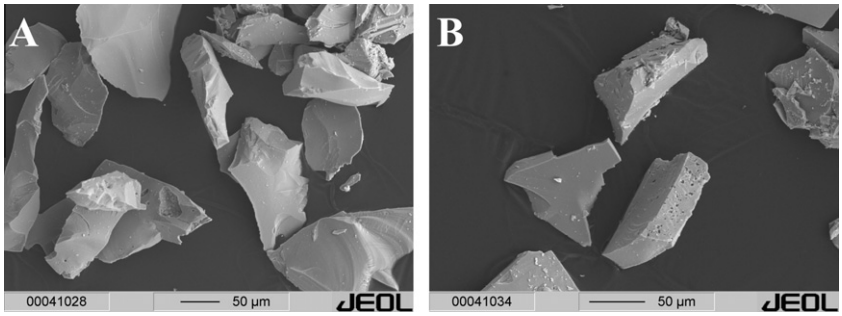

Fig. 1. SEM pictures at the end of the experiments after 201 days of oxidation (A: control experiment; B: experiment with injection of 1000 μL ^{18}O-enriched O_2). Both experiments were performed with $\delta^{18}O_{H_2O} = -8.9‰$.

Table 1
Measured DO concentrations and calculated absolute O_2 amounts in the aqueous and gaseous phase (estimated with Henry's law) at the beginning of the experiments and at the end after 201 days.

Volume of $\delta^{18}O_{O_2}$ injection (μL)	$^{18}O_2$ injection (mmol)	DO (mmol L^{-1})	DO (mmol)	O_2 in headspace (mmol)	O_2 in total system (mmol)	O_2 consumption (mmol)
Initial values at the beginning of the experiments						
		0.2334	0.0584	2.211	2.270	
Experiments with initial $\delta^{18}O_{H_2O} = -17.5‰$ *(after 201 d)*						
0 (control)	0	0.0548	0.0137	0.520	0.533	−1.736
250	0.0022	0.0549	0.0137	0.520	0.534	−1.735
500	0.0044	0.0463	0.0116	0.438	0.450	−1.820
1000	0.0087	0.0536	0.0134	0.508	0.521	−1.748
Experiments with initial $\delta^{18}O_{H_2O} = -8.9‰$ *(after 201 d)*						
0 (control)	0	0.0544	0.0136	0.515	0.529	−1.741
250	0.0022	0.0656	0.0164	0.621	0.637	−1.632
500	0.0044	0.0586	0.0146	0.555	0.570	−1.700
1000	0.0087	0.0547	0.0137	0.518	0.531	−1.738
Mean (±1σ)		0.0554 ± 0.0054	0.0138 ± 0.0013	0.524 ± 0.051	0.538 ± 0.052	−1.731 ± 0.052

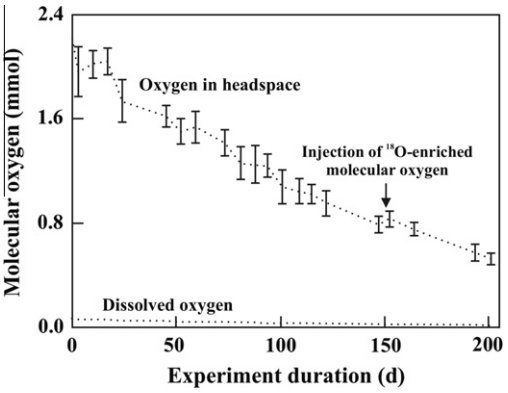

Fig. 2. Average absolute amount of O_2 in the aqueous solution and in the headspace during the experiments (error bars: 1σ, $n = 8$, error bars of dissolved O_2 are smaller than the graph).

cause SO_4^{2-} concentrations (4.62 ± 0.14 (1σ, $n = 8$) mmol L^{-1}, see Table 2) from all experiments did not differ significantly.

Ferrous iron accounted for 97–100% of the total Fe in all experiments. The molar ratio of SO_4^{2-}/total Fe was nearly stoichiometric (2.1–2.3) which indicated the lack of significant amounts of intermediate S species. Additionally, dissolved intermediate S species sulfite and thiosulfate could not be detected in any experiment, i.e., concentrations were below the detection limit of 0.001 mmol L^{-1} and 0.004 mmol L^{-1}, respectively.

3.3. Isotopes

The injection of ^{18}O-enriched O_2 into the headspace of the vessels resulted in increasing $\delta^{18}O_{O_2}$ values with increasing volume of injection (Table 3, Fig. 3). However, $\delta^{18}O_{O_2}$ values in experiments with different $\delta^{18}O_{H_2O}$ values but the same injection volume varied. This variation can be attributed to minimal variations of injection volumes due to a blockage of the syringe needle with septum "crumbs". Furthermore, injected ^{18}O-enriched O_2 may be unequally distributed within the headspace because mixing was not actively supported. However, this effect should be negligible due to rapid diffusion processes in gases.

Different $\delta^{18}O_{O_2}$ values from both control experiments without injection of ^{18}O-enriched O_2 are attributed to a technical error: headspace gas of the control experiment with $\delta^{18}O_{H_2O} = -8.9‰$ was mixed with air-O_2 during the measurement procedure of the $\delta^{18}O_{O_2}$ value. Hence, the $\delta^{18}O_{O_2}$ value was lowered and did not reflect the "true" $\delta^{18}O_{O_2}$ value of this control experiment.

$\delta^{18}O_{SO_4}$ values clearly increased with increasing volume of ^{18}O-enriched O_2 injection and $\delta^{18}O_{H_2O}$ values also seemed to increase slightly with increasing injection volume (Fig. 3). The difference between O isotopes of SO_4^{2-} and water ($\Delta^{18}O_{SO_4-H_2O}$) was 4.8‰ and 4.1‰ in control experiments with $\delta^{18}O_{H_2O} = -17.5‰$ and $\delta^{18}O_{H_2O} = -8.9‰$, respectively. Thus, $\Delta^{18}O_{SO_4-H_2O}$ values were larger than recently published O isotope enrichment factors between SO_4^{2-} and water ($\varepsilon_{SO_4-H_2O} = 2.9‰$ from Balci et al., 2007; $\varepsilon_{SO_4-H_2O} = 2.6‰$ from Mazumdar et al., 2008).

$\delta^{34}S_{SO_4}$ values (Table 3) agreed (within ±0.3‰) with $\delta^{34}S_{pyrite} = 2.5‰$.

Table 2
Hydrochemical measurements at the end of the experiments after 201 days. Pyrite oxidation rates were calculated based on the measured SO_4^{2-} concentrations by means of Eq. (6).

Volume of $\delta^{18}O_{O_2}$ injection (μL)	pH	Fe^{2+} (mmol L^{-1})	Fe^{3+} (mmol L^{-1})	Fe(total) (mmol L^{-1})	SO_4^{2-} (mmol L^{-1})	Molar ratio SO_4^{2-}/Fe(total)	Rate (mol m^{-2} s^{-1})
Experiments with initial $\delta^{18}O_{H_2O} = -17.5‰$							
0 (control)	2.1	2.03	0.01	2.04	4.47	2.2	8.7×10^{-11}
250	2.1	2.00	0.03	2.03	4.46	2.2	8.7×10^{-11}
500	2.1	2.09	0.03	2.11	4.74	2.2	9.3×10^{-11}
1000	2.1	2.10	0.03	2.13	4.60	2.2	9.0×10^{-11}
Experiments with initial $\delta^{18}O_{H_2O} = -8.9‰$							
0 (control)	2.1	2.17		2.17	4.76	2.2	9.3×10^{-11}
250	2.1	2.00	0.06	2.06	4.48	2.2	8.7×10^{-11}
500	2.2	2.13	0.04	2.17	4.66	2.1	9.1×10^{-11}
1000	2.1	2.10	0.03	2.13	4.79	2.3	9.3×10^{-11}
Mean (±1σ)	2.1 ± 0.0	2.08 ± 0.06	0.03 ± 0.02	2.11 ± 0.06	4.62 ± 0.14	2.2 ± 0.0	$9.0 \pm 0.3 \times 10^{-11}$

Table 3
Isotope measurements at the end of the experiments after 201 days. $\delta^{18}O_{O_2}$ was assumed to be 23.5‰ (Kroopnick and Craig, 1972) at the beginning of the experiments. $\delta^{34}S_{pyrite}$ was determined to be 2.5 ± 0.3‰ before the experiments. $\Delta^{18}O_{SO_4-H_2O}$ values were not calculated for experiments in which $\delta^{18}O_{H_2O}$ and $\delta^{18}O_{SO_4}$ values were "disturbed" by injection of ^{18}O-enriched O_2.

Volume of $\delta^{18}O_{O_2}$ injection (μL)	$\delta^{18}O_{H_2O}$ (‰)	$\delta^{18}O_{O_2}$ (‰)	$\delta^{18}O_{SO_4}$ (‰)	$\Delta^{18}O_{SO_4-H_2O}$ (‰)	$\delta^{34}S_{SO_4}$ (‰)
Experiments with initial $\delta^{18}O_{H_2O} = -17.5$‰					
0 (control)	−17.5	36	−12.7	4.8	2.8
250	−17.3	86	−6.1	–	2.8
500	−17.2	113	−0.9	–	2.6
1000	−17.1	248	11.1	–	2.5
Experiments with initial $\delta^{18}O_{H_2O} = -8.9$‰					
0 (control)	−8.8	28	−4.7	4.1	2.1
250	−8.8	83	1.9	–	2.5
500	−8.6	139	6.8	–	2.4
1000	−8.4	286	21.5	–	2.5

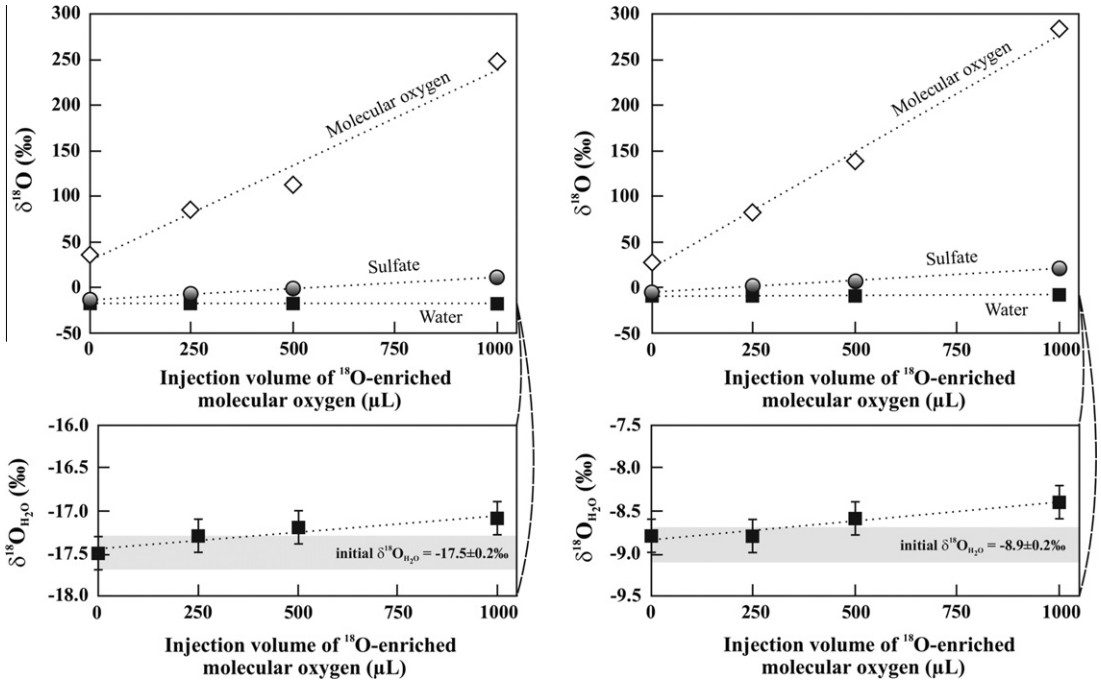

Fig. 3. $\delta^{18}O$ values of O_2 (in headspace), SO_4^{2-}, and water after 201 days of oxidation in experiments with $\delta^{18}O_{H_2O} = -17.5$‰ (left) and $\delta^{18}O_{H_2O} = -8.9$‰ (right). Top: long-term reproducibility (1σ) is smaller than symbols. Bottom: long-term reproducibility of $\delta^{18}O_{H_2O}$ values is shown ($1\sigma = 0.2$‰).

4. Discussion

4.1. Reaction rates

Almost equal pH, DO, SO_4^{2-} and Fe concentrations in all experiments showed that injected ^{18}O-enriched O_2 amounts were too low to affect oxidation rates. The absence of obvious differences between pyrite from experiments with different injection volumes of ^{18}O-enriched O_2 (Fig. 1) also indicated that the O_2 injection did not affect the oxidation intensity. Hence, the injection of ^{18}O-enriched O_2 into the headspace only affected O isotope compositions.

A lot of O_2 (Table 1: 1.632–1.820 mmol) was consumed during pyrite oxidation over 201 days. Kamei and Ohmoto (2000) observed that the rate of DO consumption during pyrite oxidation increased with increasing pyrite surface area/water volume ratio. Thus, the relatively strong decrease of DO concentrations in the present experiments may be attributed to the high surface area/water volume ratio (about 7 $m^2\,L^{-1}$) which was chosen because experimental conditions should be comparable to previous experiments from Tichomirowa and Junghans (2009) and Heidel et al. (2009). However, this surface area/water volume ratio is unusually high compared with other pyrite oxidation studies (e.g., Balci et al., 2007: 1.1 $m^2\,L^{-1}$) which may play an important role during the experiments.

Williamson and Rimstidt (1994) compiled data of several pyrite oxidation experiments and derived the following rate laws for pyrite oxidation by O_2 and Fe^{3+} (in the presence of DO) which are applicable over 4 and 6 orders of magnitude in DO and Fe^{3+} and Fe^{2+} concentrations, respectively:

$$r = 10^{-8.19}\left(m_{DO}^{0.5}\cdot m_{H+}^{-0.11}\right)\ (\text{mol m}^{-2}\ \text{s}^{-1}) \quad (7)$$

$$r = 10^{-6.07}\left(m_{Fe(III)}^{0.93}\cdot m_{Fe(II)}^{-0.40}\right)\ (\text{mol m}^{-2}\ \text{s}^{-1}). \quad (8)$$

m_{DO}, m_{H+}, $m_{(Fe(III))}$, and $m_{Fe(II)}$ are the DO, proton, Fe^{3+}, and Fe^{2+} concentrations. Table 4 shows the calculated reaction rates for the oxidation of pyrite by O_2 (reaction (1)) and Fe^{3+} (reaction (2)) which is based on the measured pH and DO, Fe^{2+} and Fe^{3+} concentrations after 201 days (from Tables 1 and 2). The obtained reaction rate of pyrite oxidation by Fe^{3+} ($r = 6.8 \pm 2.6 \times 10^{-10}$ (1σ, $n = 8$)

Table 4
Reaction rates for pyrite oxidation by O_2 and by Fe^{3+} and Fe^{2+} oxidation calculated from measured concentrations after 201 days (shown in Table 1) by means of Eqs. (7)–(9).

Volume of $\delta^{18}O_{O_2}$ injection (μL)	FeS_2 oxidation by O_2 (mol m^{-2} s^{-1})	FeS_2 oxidation by Fe^{3+} (mol m^{-2} s^{-1})	Fe^{2+} oxidation (mol L^{-1} s^{-1})
Experiments with initial $\delta^{18}O_{H_2O} = -17.5‰$			
0 (control)	8.2×10^{-11}	3.2×10^{-10}	1.4×10^{-13}
250	8.2×10^{-11}	6.1×10^{-10}	1.4×10^{-13}
500	7.5×10^{-11}	6.0×10^{-10}	1.2×10^{-13}
1000	8.1×10^{-11}	6.0×10^{-10}	1.4×10^{-13}
Experiments with initial $\delta^{18}O_{H_2O} = -8.9‰$			
0 (control)	8.1×10^{-11}	n.d.[a]	1.5×10^{-13}
250	9.0×10^{-11}	1.2×10^{-9}	1.7×10^{-13}
500	8.5×10^{-11}	8.6×10^{-10}	1.6×10^{-13}
1000	8.1×10^{-11}	6.0×10^{-10}	1.5×10^{-13}
Mean (±1σ)	$8.2 \pm 0.4 \times 10^{-11}$	$6.8 \pm 2.6 \times 10^{-10}$	$1.5 \pm 0.1 \times 10^{-13}$

[a] Rate could not be determined because the ferric iron concentration was below the detection limit.

mol m^{-2} s^{-1}) was about one order of magnitude faster than the reaction rate of pyrite oxidation by O_2 ($r = 8.2 \pm 0.4 \times 10^{-11}$ (1σ, $n = 8$) mol m^{-2} s^{-1}). Accordingly, Fe^{3+} should be the dominating oxidant (electron acceptor) of pyrite after 201 days of oxidation as is commonly proposed for acid pH conditions (e.g., Nordstrom, 1982).

Changing conditions (DO, Fe^{2+} and Fe^{3+} concentrations, pH) may result in changing reaction rates over 201 days of oxidation. Therefore, reaction rates of pyrite oxidation by O_2 were estimated by means of measured DO concentrations during the experiments and linear interpolated proton concentrations. According to Eq. (7), decreasing DO concentrations and decreasing pH caused a decrease of the reaction rate from $1.8 \pm 0.05 \times 10^{-10}$ (1σ, $n = 8$) mol m^{-2} s^{-1} (after 3 days) to $8.2 \pm 0.4 \times 10^{-11}$ (1σ, $n = 8$) mol m^{-2} s^{-1} after 201 days which is shown as a surface-normalized reaction rate (multiplied by specific surface area and pyrite mass) in Fig. 4. Considering changing reaction rates, 3.1 mmol pyrite (cumulative amount of oxidized pyrite according to calculated reaction rates) should be oxidized by O_2 within 201 days. According to reaction (1), 11.0 mmol DO should be consumed and 6.3 mmol SO_4^{2-} should be produced within 201 days, which exceeds the measured concentrations (Table 1: 1.632–1.820 mmol O_2 consumed, Table 2: 1.11–1.20 mmol SO_4^{2-} produced). Hence, calculations with rate law (7) resulted in overestimated oxidation rates.

The rate of pyrite oxidation by Fe^{3+} could only be calculated for day 201 (Fig. 4), where Fe^{2+} and Fe^{3+} concentrations were known. It may have changed during the experiments due to increasing Fe^{2+} and, thus, Fe^{3+} concentrations.

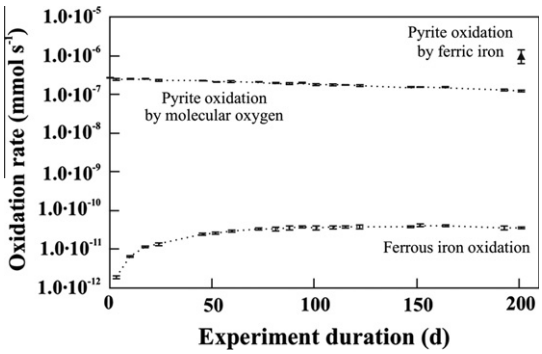

Fig. 4. Reaction rates of pyrite oxidation by O_2 and Fe^{3+} and Fe^{2+} oxidation during the experiments calculated by means of Eqs. (7)–(9) (error bars: 1σ, $n = 8$, see text for calculation). Note the logarithmic scale of the *y*-axis.

The rate of Fe^{2+} oxidation by O_2 under acid pH conditions can be estimated by the following equation from Singer and Stumm (1970):

$$r = k' \cdot m_{Fe(II)} \cdot p_{O_2} \left(\text{mol L}^{-1}\ \text{s}^{-1}\right), \quad (9)$$

where $k' = 1.0 \times 10^{-7}$ atm^{-1} min^{-1} at 25 °C, $m_{Fe(II)}$ is the Fe^{2+} concentration, and p_{O_2} is the partial pressure of O_2. Table 4 shows the reaction rate of the Fe^{2+} oxidation (reaction (3)) which was calculated by means of Eq. (9) with the measured Fe^{2+} and DO concentrations after 201 days. The obtained rate ($1.5 \pm 0.1 \times 10^{-13}$ (1σ, $n = 8$) mol L^{-1} s^{-1}) indicated that the Fe^{2+} oxidation by O_2 was very slow after 201 days due to acid pH conditions and relatively low DO concentrations. The initial Fe^{2+} oxidation rate should be even slower ($7.9 \pm 0.8 \times 10^{-15}$ (1σ, $n = 8$) mol L^{-1} s^{-1}, based on measured DO concentrations after 3 days and interpolated Fe^{2+} concentrations). Volume-normalized reaction rates (multiplied by solution volume) in Fig. 4 show that the Fe^{2+} oxidation rate increased during the experiments (due to increasing Fe^{2+} concentrations) until it remained more or less constant (due to simultaneously decreasing DO concentrations) after about 90 days (based on measured DO concentrations and linear interpolated Fe^{2+} concentrations).

Considering that the experiments were performed with 250 mL aqueous solution, only 0.001 mmol Fe^{2+} should be oxidized within 201 days. According to reaction (3), only 0.001 mmol Fe^{3+} should be produced which is lower than measured Fe^{3+} concentrations after 201 days (Table 2: 0.01–0.06 mmol L^{-1} equals 0.004–0.014 mmol). Presumably, more Fe^{3+} may be produced than calculated by means of Eq. (9) which was derived from experiments with dissolved Fe^{2+} in the absence of pyrite (Singer and Stumm, 1970). Bonnissel-Gissinger et al. (1998) concluded from their experiments that the Fe^{2+} oxidation may be catalyzed on the pyrite surface. Due to the lack of an exact determination of the Fe^{3+} production during the experiments, a potential change of the reaction rate of pyrite oxidation by Fe^{3+} cannot be calculated.

In conclusion, calculations with the rate law from Williamson and Rimstidt (1994) resulted in an overestimated rate of pyrite oxidation by O_2. However, it could be shown that the rate of pyrite oxidation by O_2 slowed down during the experiments. Pyrite oxidation by Fe^{3+} (calculated by the rate law of Williamson and Rimstidt (1994)) was faster than pyrite oxidation by O_2 after 201 days; but no information could be obtained about a potential change of the rate during the experiments. Calculations with the rate law from Singer and Stumm (1970) resulted in an underestimated rate of Fe^{2+} oxidation. A comparison of reaction rates calculated from rate laws (7) and (9) indicated that less O_2 should be consumed during Fe^{2+} oxidation compared with pyrite oxidation by O_2. Hence, it remains uncertain from calculated reactions rates if O_2 is primarily consumed (i.e., reduced) during pyrite oxidation or during Fe^{2+} oxidation which would then result in pyrite oxidation by Fe^{3+}.

4.2. Oxygen isotope enrichment factor between sulfate and molecular oxygen ($\varepsilon_{SO_4-O_2}$)

The remaining O_2 in the aqueous solution and in the headspace became isotopically heavier even in control experiments (Table 3) which indicated the preferential consumption of ^{16}O during the oxidation experiments. Hence, $\delta^{18}O_{O_2}$ values had already been increased in all experiments before ^{18}O-enriched O_2 was injected after 151 days. $\delta^{18}O_{O_2}$ values can be calculated by means of a modified Rayleigh fractionation trend (Oba and Poulson, 2009a):

$$\ln\left(\frac{\delta^{18}O_{O_2} + 1000}{\delta^{18}O_{\text{initial}\,O_2} + 1000}\right) \times 1000 = \varepsilon_{SO_4-O_2} \ln f, \quad (10)$$

where $\delta^{18}O_{initial\,O_2}$ is the $\delta^{18}O_{O_2}$ value at the beginning of the experiments, $\varepsilon_{SO_4-O_2}$ is the O isotope enrichment factor between SO_4^{2-} and O_2, and f is the fraction of remaining O_2. Calculations with $\delta^{18}O_{initial\,O_2} = 23.5‰$ (Kroopnick and Craig, 1972), $\varepsilon_{SO_4-O_2} = -9.8‰$ (Balci et al., 2007), and f calculated from measured DO concentrations after 150 days resulted in a theoretical $\delta^{18}O_{O_2}$ value of 33.9 ± 0.8‰ (1σ, $n = 8$).

From 151 to 201 days, $\delta^{18}O_{O_2}$ values increased further in all experiments due to the preferential consumption of ^{16}O during pyrite oxidation. In addition, $\delta^{18}O_{O_2}$ values increased in experiments where ^{18}O-enriched O_2 was injected. Hence, increasing $\delta^{18}O_{O_2}$ values in control experiments resulted only from preferential ^{16}O consumption, whereas increasing $\delta^{18}O_{O_2}$ values in experiments with injection of ^{18}O-enriched O_2 resulted from preferential ^{16}O consumption and injection of ^{18}O-enriched O_2.

After 201 days, a theoretical $\delta^{18}O_{O_2}$ value of 38.2 ± 0.1‰ (1σ, $n = 8$) was calculated by means of Eq. (10) for the control experiments. The measured $\delta^{18}O_{O_2}$ value of 36‰ (from the control experiment with $\delta^{18}O_{H_2O} = -17.5‰$) was slightly lower than the theoretical $\delta^{18}O_{O_2}$ value. (The measurement of the $\delta^{18}O_{O_2}$ value from the control experiment with $\delta^{18}O_{H_2O} = -8.9‰$ failed due the reason mentioned in Section 3.3.) According to Eq. (10), $\varepsilon_{SO_4-O_2}$ equals the slope of a regression line which is defined by the initial values ($f = 1$, $\delta^{18}O_{O_2} = \delta^{18}O_{initial\,O_2} = 23.5‰$) and the measured values at the end of the experiments after 201 days ($f < 0.23$, $\delta^{18}O_{O_2} = 36‰$). $\varepsilon_{SO_4-O_2}$ was determined to be −8.4‰ from the control experiment with $\delta^{18}O_{H_2O} = -17.5‰$ (Fig. 5). However, $\varepsilon_{SO_4-O_2} = -8.4‰$ should be regarded as a rough estimation because it is based on only one control experiment with only two values forming a regression line.

The O isotope enrichment in SO_4^{2-} compared with O_2 may be caused by two O consumption processes: O_2 reduction during pyrite oxidation and during oxidation of Fe^{2+}. Oba and Poulson (2009a) investigated the O isotope enrichment of DO that occurs during O_2 consumption by sodium sulfide oxidation. They determined a range of $\varepsilon_{SO_4-O_2}$ between −10.9‰ and −10.3‰ (at neutral pH and 23 °C) and observed that the $\varepsilon_{SO_4-O_2}$ value does not depend on sulfide concentration and temperature. Oba and Poulson (2009a) suggested that the reaction mechanism (and $\varepsilon_{SO_4-O_2}$) of sodium sulfide oxidation may depend on pH and concluded that $\varepsilon_{SO_4-O_2}$ should only be valid and comparable for the same pH conditions. Nevertheless, the $\varepsilon_{SO_4-O_2}$ of −8.4‰ obtained in the present study from pyrite oxidation under acid pH conditions agrees with the $\varepsilon_{SO_4-O_2}$ obtained from aqueous sodium sulfide oxidation at neutral pH (Lloyd, 1967: −8.7‰; Oba and Poulson, 2009a: −10.9 to −10.3‰) as well as with $\varepsilon_{SO_4-O_2}$ obtained from previous pyrite oxidation experiments at acid pH (Balci et al., 2007: −9.8‰). Taylor et al. (1984) observed a smaller $\varepsilon_{SO_4-O_2}$ of −4.3‰ from abiotic pyrite oxidation experiments at pH 2 and 30 °C under a pure O_2 atmosphere and a larger $\varepsilon_{SO_4-O_2}$ of −11.4‰ from similar experiments with *Acidithiobacillus ferrooxidans*. However, Balci et al. (2007) observed no significant differences between $\varepsilon_{SO_4-O_2}$ from abiotic (−9.8‰) and biotic pyrite oxidation experiments with *A. ferrooxidans* (−10.0‰ and −10.8‰) from their experiments with continuously sparged O_2-saturated air.

In comparison, the reduction of O_2 during the oxidation of 0.17 mol L^{-1} dissolved Fe^{2+} to Fe^{3+} was associated with an O isotope enrichment factor of −11.6‰ at acid pH and 23 °C (Oba and Poulson, 2009b). This ε value is similar to the O isotope enrichment that occurs during pyrite oxidation (Balci et al., 2007; this work). Oba and Poulson (2009b) observed that the O isotope enrichment factor became larger with decreasing Fe^{2+} concentration under acid pH conditions (23 °C: from −5.7‰ at 0.67 mol L^{-1} Fe^{3+} to −11.6‰ at 0.17 mol L^{-1} Fe^{3+}). Presumably, the O isotope enrichment factor in the present experiments would have been larger if the oxidation of the relatively low amount of dissolved Fe^{2+} (2.08 ± 0.06 mmol L^{-1} (1σ, $n = 8$) after 201 days) had been the dominating O_2 consumption process. Hence, the O isotope enrichment factor $\varepsilon_{SO_4-O_2} = -8.4‰$ from the abiotic oxidation experiments under acid conditions may indicate that O_2 was predominantly consumed during pyrite oxidation. Furthermore, O_2 may be consumed during oxidation of Fe^{2+} which was adsorbed onto the pyrite surface.

4.3. Relative proportion of molecular oxygen in sulfate in aerobic experiments

Heidel et al. (2009) observed a constant difference between $\delta^{18}O_{SO_4}$ and $\delta^{18}O_{H_2O}$ values ($\Delta^{18}O_{SO_4-H_2O}$) of 3.3–4.0‰ from aerobic long-term experiments (150–300 days) with similar conditions. This $\Delta^{18}O_{SO_4-H_2O}$ value was in the range of published $\varepsilon_{SO_4-H_2O}$ values (0.0–4.0‰). Hence, it reflected either the O isotope enrichment factor $\varepsilon_{SO_4-H_2O}$ or – in addition to $\varepsilon_{SO_4-H_2O}$ – a small amount of O_2 which was incorporated into SO_4^{2-}. Heidel et al. (2009) preferred the latter interpretation, but they were not able to confirm their hypothesis. Now, increasing $\delta^{18}O_{SO_4}$ values with increasing injection of ^{18}O-enriched O_2 in the present experiments have shown that O_2 is definitely incorporated into SO_4^{2-} even after more than 151 days of oxidation.

Relative proportions of O_2 and water-derived O in SO_4^{2-} were calculated by means of the general isotope-balance model (Eq.

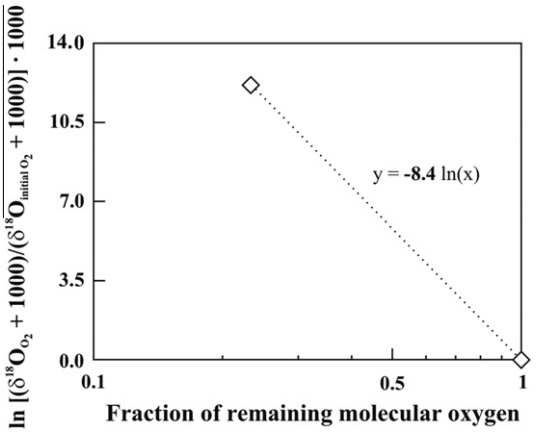

Fig. 5. Regression of ln $[(\delta^{18}O_{O_2} + 1000)/(\delta^{18}O_{initial\ O_2} + 1000)] \times 1000$ vs. fraction of remaining O_2 from the control experiment with $\delta^{18}O_{H_2O} = -17.5‰$. The slope equals the O isotope enrichment factor between SO_4^{2-} and O_2 ($\varepsilon_{SO_4-O_2}$).

Table 5
Relative proportion of molecular oxygen in sulfate calculated from measured $\delta^{18}O_{SO_4}$, $\delta^{18}O_{O_2}$, and $\delta^{18}O_{H_2O}$ values after 201 days (shown in Table 3) and different O isotope enrichment factors $\varepsilon_{SO_4-O_2}$ and $\varepsilon_{SO_4-H_2O}$ by means of the general isotope-balance model (Eq. (4)).

Volume of $\delta^{18}O_{O_2}$ injection (μL)	Proportion of O_2 in SO_4^{2-} (%) using		
	$\varepsilon_{SO_4-O_2} = -4.3‰$ and $\varepsilon_{SO_4-H_2O} = 0.0‰$ (Taylor and Wheeler, 1994)	$\varepsilon_{SO_4-O_2} = -9.8‰$ and $\varepsilon_{SO_4-H_2O} = 2.9‰$ (Balci et al., 2007)	$\varepsilon_{SO_4-O_2} = -8.4‰$ (this work) and $\varepsilon_{SO_4-H_2O} = 2.9‰$ (Balci et al., 2007)
Experiments with initial $\delta^{18}O_{H_2O} = -17.5‰$			
0 (control)	10	5	5
250	11	9	9
500	13	11	11
1000	11	10	10
Experiments with initial $\delta^{18}O_{H_2O} = -8.9‰$			
0 (control)	13	5	5
250	12	10	10
500	11	9	9
1000	10	10	10
Mean (±1σ)	11 ± 1	9 ± 2	8 ± 2

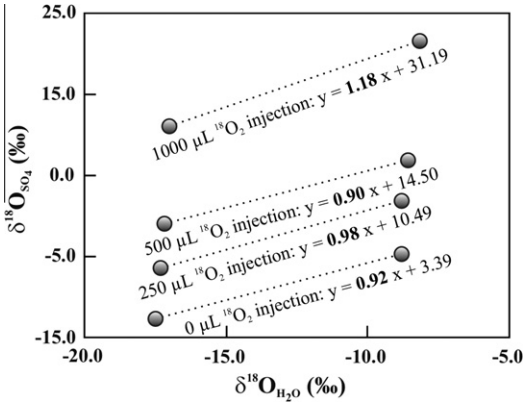

Fig. 6. Linear fit of $\delta^{18}O_{SO_4}$ values vs. $\delta^{18}O_{H_2O}$ values at day 201. The slope equals the proportion of water-derived O in SO_4^{2-}. Long-term reproducibility (1σ) is smaller than symbols.

(4)) using the measured $\delta^{18}O_{SO_4}$, $\delta^{18}O_{O_2}$, and $\delta^{18}O_{H_2O}$ values after 201 days and different O isotope enrichment factors $\varepsilon_{SO_4-O_2}$ and $\varepsilon_{SO_4-H_2O}$ (Table 5). They should be regarded as rough estimations due to changing $\delta^{18}O_{O_2}$ values during the experiments. The proportion of O_2 in SO_4^{2-} ranged from 5% to 13%; but average proportions of O_2 in SO_4^{2-} showed a smaller range of 8–11% (Table 5). Differences in the relative proportions resulted from the use of different O enrichment factors $\varepsilon_{SO_4-O_2}$ and $\varepsilon_{SO_4-H_2O}$.

The relative proportions of O from both sources in SO_4^{2-} could also be estimated without knowledge of $\varepsilon_{SO_4-O_2}$ and $\varepsilon_{SO_4-H_2O}$ by linear fit of $\delta^{18}O_{SO_4}$ values vs. $\delta^{18}O_{H_2O}$ values (Fig. 6). The slope of the line equals the water-derived O proportion in SO_4^{2-} (e.g., Gould et al., 1989; Balci et al., 2007; Nordstrom et al., 2007). Control experiments gave 92% water-derived O and 8% O_2 in SO_4^{2-} which agrees with the estimated relative proportions using the general isotope-balance model. The results from experiments with injection of 250 µL and 500 µL ^{18}O-enriched O_2 (98% and 90% water-derived O in SO_4^{2-}, respectively) were similar to the control experiments. However, experiments with 1000 µL ^{18}O-enriched O_2 injection gave 118% water-derived O in SO_4^{2-}. This questionable result may indicate that $\delta^{18}O_{O_2}$ values and, thus, $\delta^{18}O_{SO_4}$ values varied due to minimal variations of injection volumes of ^{18}O-enriched O_2 (see Section 3.3). The linear fit method requires identical conditions ($\delta^{18}O_{O_2}$ values) for experiments with different $\delta^{18}O_{H_2O}$ values. Otherwise the slope of the line can give inaccurate results. Furthermore, the limited dataset (slope based on only two values) and analytical limitations contributed to the doubtful proportion of 118% water-derived O in SO_4^{2-}.

The mean of all calculations (from Table 5 and Fig. 6 except of experiments with 1000 µL ^{18}O-enriched O_2 injection) indicated that 9 ± 3% (1σ, $n = 27$) O_2 oxygen (and, thus, 91% water-derived O) was incorporated into SO_4^{2-} after more than 151 days of pyrite oxidation.

4.4. Reaction mechanisms

Pyrite oxidation is an electrochemical process that consists of several oxidation–reduction reactions (release and acceptance of electrons). The observed increase in $\delta^{18}O_{SO_4}$ and $\delta^{18}O_{H_2O}$ values with increasing injection volume of ^{18}O-enriched O_2 as well as hydrochemical investigations allow conclusions on pyrite oxidation mechanisms.

4.4.1. Molecular oxygen consumption during cathodic reactions of pyrite oxidation

During cathodic reactions, electrons are transferred from pyrite to the electron acceptor which may be O_2 and Fe^{3+}. Furthermore, O_2 may accept electrons from Fe^{2+} during the oxidation to Fe^{3+}. The cathodic reactions can be described by (e.g., Holmes and Crundwell, 2000; Rimstidt and Vaughan, 2003):

$$0.5O_2 + 2H^+ + 2e^- \rightarrow H_2O \quad (11)$$

$$Fe^{3+} + e^- \rightarrow Fe^{2+}. \quad (12)$$

Additionally, O_2 may be reduced by:

$$O_2 + 4e^- \rightarrow 2O^{2-}. \quad (13)$$

Based on the calculated relative proportion of 9 ± 3% (1σ) O_2 in SO_4^{2-}, an absolute amount of 0.069 ± 0.002 (1σ, $n = 8$) mmol O_2 was incorporated into the produced SO_4^{2-} (4.62 ± 0.14 (1σ, $n = 8$) mmol L^{-1} from Table 2) during the experiments. Considering that 1.731 ± 0.052 (1σ, $n = 8$) mmol O_2 was consumed after 201 days (see Table 1), only 4.0 ± 0.1% (1σ, $n = 8$) of the consumed O_2 was incorporated into the produced SO_4^{2-}. Thus, most of the O_2 (remaining 1.662 ± 0.051 (1σ, $n = 8$) mmol) must be consumed by an additional mechanism. Slightly increased $\delta^{18}O_{H_2O}$ values in experiments with the greatest injection of ^{18}O-enriched O_2 indicated that O_2 may be consumed by incorporation into water molecules. This mechanism could occur according to reaction (11), i.e., O_2 accepts electrons from pyrite and/or Fe^{2+}. Thus, O_2 together with protons forms water molecules.

According to reaction (11), the cathodic reduction of 1.662 mmol O_2 would produce 3.32 ± 0.10 (1σ, $n = 8$) mmol water which was mixed with the initial amount of 13,864 mmol water (250 mL at 20 °C). The measured $\delta^{18}O_{H_2O}$ value after 201 days should be a mixture of the initial $\delta^{18}O_{H_2O}$ value and the $\delta^{18}O_{H_2O}$ value of the newly formed water:

$$\delta^{18}O_{H_2O} = Y \cdot \delta^{18}O_{H_2O}\,(\text{initial}) + (1 - Y)\delta^{18}O_{H_2O}\,(\text{newly formed}), \quad (14)$$

where $\delta^{18}O_{H_2O}$ (initial) is the initial $\delta^{18}O_{H_2O}$ value (−17.5‰ and −8.9‰), $\delta^{18}O_{H_2O}$ (newly formed) is the $\delta^{18}O_{H_2O}$ value of water formed from O_2 and protons, and Y and $(1 - Y)$ are the relative proportions of the initial and the newly formed water, respectively. Even if all newly formed water were to be produced with ^{18}O-enriched O_2 (which was not the case because ^{18}O-enriched O_2 was not injected at the beginning of the experiments but after 151 days), the greatest injection of 1000 µL ^{18}O-enriched O_2 should not result in an increase of the initial $\delta^{18}O_{H_2O}$ value. Calculations with rearrangement of Eq. (14) indicate that at least 20 mmol water with ^{18}O-enriched O_2 is required to achieve the observed increase in $\delta^{18}O_{H_2O}$ values. Hence, at least 10 mmol O_2 should be consumed according to Eq. (11). However, only 2.270 mmol O_2 was available in the whole system (aqueous and gaseous phase). Thus, stoichiometric calculations failed.

However, the incorporation into water molecules of O_2 during its cathodic reduction (reaction (11)) seems to be the only logical explanation for the observed increase in $\delta^{18}O_{H_2O}$ values in experiments with the highest injection of ^{18}O-enriched O_2. Increasing $\delta^{18}O_{H_2O}$ values cannot be caused by evaporation because no leakage was observed which is supported by decreasing DO concentrations. (If the system was leaky, DO concentrations must not decrease.)

Although reaction (11) suggests the consumption of protons, the observed pH decrease may be explained by simultaneously proceeding anodic reactions which result in proton production (see Section 4.4.2).

Krouse et al. (1991) performed pentlandite ($(Fe, Ni)_9S_8$) oxidation experiments with injection of ^{18}O-enriched O_2 and observed its incorporation into water (and SO_4^{2-}) during biotic experiments with *Thiobacillus ferrooxidans*. However, O_2 was not incorporated

into water during abiotic control experiments although much larger injection volumes of O_2 with much higher $\delta^{18}O_{O_2}$ values were used compared with the present experiments. No information was given about the amounts of produced SO_4^{2-} and the $\delta^{18}O_{SO_4}$ values during the abiotic experiments (Krouse et al., 1991). A low oxidation rate in abiotic experiments may explain the lack of incorporation of ^{18}O-enriched O_2 into water; but no information was given for this experiment. Hence, the present results may not contradict the results of Krouse et al. (1991).

Calculated reaction rates could not give reliable information about the dominating reactions. Hence, O_2 may be reduced by electron acceptance from pyrite (reaction (1)) and/or Fe^{2+} (reaction (3)). The observed O isotope enrichment factor $\varepsilon_{SO_4-O_2}$ may indicate that the oxidation of dissolved Fe^{2+} was not a dominating process during the experiments. Accordingly, the production of dissolved Fe^{3+} was low (Table 2: 0.02–0.06 mmol L^{-1} after 201 days).

The oxidation of adsorbed Fe^{2+} to Fe^{3+} may be catalyzed on the pyrite surface (Bonnissel-Gissinger et al., 1998). However, Thurston et al. (2010) suggested from their chalcopyrite oxidation experiments and previous pyrite oxidation studies that ^{32}S is enriched in SO_4^{2-} compared to the sulfide during abiotic sulfide oxidation by Fe^{3+}. Accordingly, the lack of S isotope enrichment between SO_4^{2-} and pyrite (Table 3) may indicate that pyrite oxidation by Fe^{3+} played no important role in the present experiments under abiotic acid conditions. Thus, more O_2 should be consumed during pyrite oxidation than during adsorbed Fe^{2+} oxidation which would then result in pyrite oxidation by Fe^{3+}. The formation of O anions by reaction (13) should proceed simultaneously to reaction (11) but at a lower rate. Oxygen anions may be incorporated into SO_4^{2-} as shown in the next section.

4.4.2. Molecular oxygen incorporation into sulfate during anodic reactions of pyrite oxidation

At the anodic site, electrons are removed from S sites stepwise (and transferred to the cathodic site due to the semiconductivity of pyrite) and O_2 reacts with pyrite–S to form SO_4^{2-}. Rosso et al. (1999), Rimstidt and Vaughan (2003), and Rosso and Vaughan (2006) proposed a mechanism for the incorporation of water-derived O into SO_4^{2-} during the anodic reaction. According to this model, O_2 is dissociated and adsorbed on pyrite–Fe sites and makes the nearby pyrite–S sites more susceptible for hydroxyl attack from dissociated water which can be described by the following reaction (Rimstidt and Vaughan, 2003):

$$Fe—S—S + H_2O \rightarrow Fe—S—S—O + 2H^+ + 2e^-. \quad (15)$$

Reaction (15) is repeated until pyrite–S is completely oxidized to SO_4^{2-}. According to this model, water-derived O (via hydroxyls) but no O_2 is incorporated into SO_4^{2-} during the anodic reaction.

However, a parallel anodic reaction with incorporation of O_2 into SO_4^{2-} must occur because 4.0 ± 0.1% (1σ, n = 8) of the consumed O_2 was incorporated into the produced SO_4^{2-} during the pyrite oxidation experiments. This incorporation may occur by the following mechanisms: (i) via water in which O_2 is incorporated due to cathodic reaction (11), (ii) via direct reaction with S sites of pyrite, (iii) via sulfite oxidation, or (iv) via tetrathionate oxidation.

4.4.2.1. Indirect incorporation of molecular oxygen into sulfate via incorporation into water during the cathodic reduction of molecular oxygen. The incorporation of ^{18}O-enriched O_2 into water is indicated by a slight increase in $\delta^{18}O_{H_2O}$ values in experiments with injection of 1000 µL ^{18}O-enriched O_2. In contrast, the rise in $\delta^{18}O_{SO_4}$ values is obviously higher (Table 3, Fig. 3). Hence, the increase of $\delta^{18}O_{SO_4}$ values cannot only be caused by the incorporation of ^{18}O-enriched water-derived oxygen but must be caused by another mechanism.

4.4.2.2. Direct reaction of molecular oxygen with sulfur sites of pyrite. Tichomirowa and Junghans (2009) proposed a mechanism where O_2 is adsorbed on S sites of pyrite and directly incorporated into SO_4^{2-} during the initial phase (first 10 days) of their pyrite oxidation experiments. Similar to reaction (15), an anodic reaction with O_2 may be simply described by:

$$Fe—S—S + O^{2-} \rightarrow Fe—S—S—O + 2e^-. \quad (16)$$

The O anion incorporated into SO_4^{2-} may be produced by the cathodic reaction (13).

Hubbard et al. (2009) also suggested the direct incorporation of O_2 via pyrite–S sites, although they mentioned that such a mechanism is not favored within the literature. Heidel et al. (2009) observed that the initial direct reaction of O_2 with pyrite–S sites occurs especially on ultrafine-grained pyrite and under acid pH conditions. Fig. 7 shows data from this work, Tichomirowa and Junghans (2009), and Heidel et al. (2009), which indicate an initial grain size-dependent (i.e., surface-controlled) mechanism of O_2 incorporation into SO_4^{2-}. Hence, O_2 could be initially incorporated into SO_4^{2-} by direct reaction with pyrite–S sites (Tichomirowa and Junghans, 2009; Heidel et al., 2009).

Later on, pyrite–S sites are only attacked by hydroxyls from dissociated water leading to decreasing $\delta^{18}O_{SO_4}$ values, i.e., a decreasing proportion of O_2 in SO_4^{2-} (Tichomirowa and Junghans, 2009; Heidel et al., 2009). Final constant $\delta^{18}O_{SO_4}$ values indicate that a grain size-independent mechanism dominates the O_2 incorporation into SO_4^{2-}. Such a mechanism should also result in the permanent incorporation of about 9 ± 3% (1σ) O_2 into SO_4^{2-} during the initial oxidation (Fig. 7). Heidel et al. (2009) proposed that O_2 is permanently incorporated into SO_4^{2-} by sulfite oxidation which is discussed below.

In conclusion, the direct reaction of O_2 with pyrite–S sites may explain the grain size-dependent incorporation of O_2 into SO_4^{2-} during the initial phase of oxidation, but cannot explain the incorporation of O_2 which was observed from 151 to 201 days in the oxidation experiments.

4.4.2.3. Incorporation of molecular oxygen into sulfate via sulfite oxidation. In the literature, the oxidation of the intermediate S species sulfite is the most favored mechanism for the incorporation of

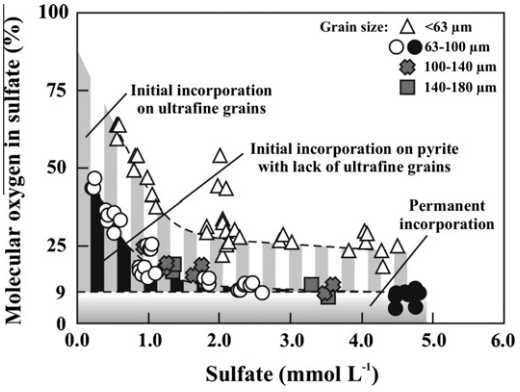

Fig. 7. Relative proportions of O_2 in SO_4^{2-} in experiments from the present work (black-filled symbols), Tichomirowa and Junghans (2009) (unfilled symbols), and Heidel et al. (2009) (grey-filled symbols) calculated by means of the general isotope-balance model with $\varepsilon_{SO_4-O_2} = -9.8‰$ and $\varepsilon_{SO_4-H_2O} = 2.9‰$ from Balci et al. (2007). All experiments were performed with same water volumes and pyrite masses at acid pH (about 2), but differ in grain size and experiment duration (from 2 to 201 days).

O_2 into SO_4^{2-}. Seal (2003) and Balci et al. (2007) proposed that the stepwise oxidation of pyrite by Fe^{3+} (as electron acceptor) produces several S intermediate species which solely contain water-derived O. Sulfite may be released into solution where it is finally oxidized to SO_4^{2-} by O_2:

$$SO_3^{2-} + 0.5O_2 \rightarrow SO_4^{2-}. \quad (17)$$

If SO_4^{2-} is exclusively produced by this pathway, it should contain 25% O_2 (and 75% water-derived O) which exceeds the observed proportion of 9 ± 3% (1σ) O_2 in SO_4^{2-}. Hence, some of the pyrite–S may be completely oxidized to SO_4^{2-} on the pyrite surface before it is released into solution. This SO_4^{2-} may contain only water-derived O according to the proposed mechanism from Rosso et al. (1999).

Sulfite could not be detected in experiments under acid pH conditions (e.g., Seal, 2003; Tichomirowa and Junghans, 2009; Heidel et al., 2009; this work) presumably due to its extremely fast oxidation. This is in agreement with the $\delta^{34}S_{SO_4}$ values which were similar to $\delta^{34}S_{pyrite}$ = 2.5‰ and indicated the short lifetime (and/or absence of) of intermediate S species (Taylor et al., 1984).

Sulfite rapidly exchanges O isotopes with water which is associated with an O isotope enrichment in sulfite compared with water (expressed as $\varepsilon_{SO_3-H_2O}$). Brunner et al. (2006) observed that $\varepsilon_{SO_3-H_2O}$ increased with decreasing pH and decreasing temperature from experiments at pH 7.2 and 8 and temperatures between 4 and 70 °C. At 23 °C, $\varepsilon_{SO_3-H_2O}$ = 11.5‰ and $\varepsilon_{SO_3-H_2O}$ = 7.9‰ were determined for pH 7.2 and 8, respectively (Brunner et al., 2006).

The O isotope composition of SO_4^{2-} formed from sulfite oxidation under suboxic, O_2-limited conditions can be estimated as follows (Seal, 2003, with data from Holt et al., 1981):

$$\delta^{18}O_{SO_4} = 0.74 \cdot \delta^{18}O_{H_2O} + 15.4. \quad (18)$$

Eq. (18) suggests that about 75% water-derived O is incorporated into SO_4^{2-} during sulfite oxidation and also includes the $\varepsilon_{SO_3-H_2O}$ value in the *y*-intercept.

The relative proportions of O_2-free SO_4^{2-} (formed according to the mechanism from Rosso et al., 1999) and O_2-containing SO_4^{2-} (formed via sulfite oxidation) can be estimated by means of a modified general isotope-balance model:

$$\delta^{18}O_{SO_4} = Z \cdot (\delta^{18}O_{H_2O} + \varepsilon_{SO_4-H_2O}) + (1 - Z) \cdot (0.74 \cdot \delta^{18}O_{H_2O} + 15.4), \quad (19)$$

where $\delta^{18}O_{SO_4}$ and $\delta^{18}O_{H_2O}$ are the measured $\delta^{18}O_{SO_4}$ and $\delta^{18}O_{H_2O}$ values after 201 days, $\varepsilon_{SO_4-H_2O}$ = 2.9‰ (Balci et al., 2007), and Z and $(1 - Z)$ are the relative proportions of O_2-free SO_4^{2-} and O_2-containing SO_4^{2-}, respectively. Calculations with both control experiments which were not influenced by injection of ^{18}O-enriched O_2 showed that 10 ± 2% (1σ, n = 2) of the produced SO_4^{2-} originated from sulfite oxidation. Considering that SO_4^{2-} formed from sulfite oxidation contains 25% O_2, 0.019 ± 0.003 (1σ, n = 2) mmol O_2 should be incorporated into the produced SO_4^{2-} which is lower than the observed amount of 0.069 ± 0.002 (1σ, n = 8) mmol O_2 incorporated into SO_4^{2-}.

Nevertheless, pyrite oxidation via dissolved sulfite oxidation may explain the incorporation of O_2 into SO_4^{2-}. Brunner et al. (2006) observed increasing $\varepsilon_{SO_3-H_2O}$ values with decreasing pH from experiments at pH 7.2 and 8, but no experiments were performed at acid pH conditions. It cannot be excluded that the $\varepsilon_{SO_3-H_2O}$ value is smaller at acid pH. Thus, the *y*-intercept in Eq. (18) may be smaller and the relative proportion of SO_4^{2-} produced by sulfite oxidation ($(1 - Z)$ in Eq. (19)) would become larger.

4.4.2.4. Incorporation of molecular oxygen into sulfate via tetrathionate oxidation. Nordstrom et al. (2007) reviewed publications concerning pyrite oxidation and concluded that – in addition to sulfite oxidation – there is only one further possible step in the oxidation mechanism that might require O_2: the oxidation of tetrathionate to SO_4^{2-}. In the presence of O_2 and excess Fe^{3+}, it can be described by the following equation (Druschel et al., 2003):

$$S_4O_6^{2-} + 3Fe^{3+} + 2.75O_2 + 4.5H_2O \rightarrow 3Fe^{2+} + 4SO_4^{2-} + 9H^+. \quad (20)$$

Assuming that all O in tetrathionate derives from water, about 34% of O in SO_4^{2-} would originate from O_2. However, no O isotope analyses were performed by these authors to verify if O_2 is incorporated into SO_4^{2-} or if it acts as an electron acceptor without being incorporated into SO_4^{2-}. Thus, tetrathionate oxidation may explain the incorporation of O_2 into SO_4^{2-} but an experimentally verification with low Fe^{3+} concentrations is necessary.

4.4.3. Consequences for the overall reaction mechanisms

Pyrite may be simultaneously oxidized by O_2 (reaction (1)) and Fe^{3+} (reaction (2)); but calculated reaction rates could not indicate a dominating reaction pathway. Additionally, Fe^{2+} is oxidized to Fe^{3+} by O_2 (reaction (3)). This reaction may be catalyzed onto the pyrite surface. Nevertheless, the reaction rate of Fe^{2+} oxidation should not be faster than that of pyrite oxidation by O_2 during the experiments under abiotic acid conditions. Otherwise, pyrite would be predominantly oxidized by Fe^{3+} and O_2 would not be incorporated into the produced SO_4^{2-}. However, O_2 is permanently incorporated into SO_4^{2-} presumably via sulfite and tetrathionate oxidation. The electron transfer from pyrite and Fe^{2+} to O_2 results in the reduction of O_2 to form water molecules.

4.5. Application to field investigations

Hubbard et al. (2009) recently discussed reasons for high $\delta^{18}O_{SO_4}$ values from field studies which indicated large contents of O_2 in SO_4^{2-} formed from pyrite oxidation. These authors explained their high $\delta^{18}O_{SO_4}$ values as being due to O isotope exchange between sulfite and water followed by sulfite oxidation to SO_4^{2-} by O_2. However, they highlighted that this mechanism could not explain the observed proportions of more than 25% O_2 in SO_4^{2-}.

The present laboratory experiments also showed that the permanent incorporation of O_2 into SO_4^{2-} via sulfite oxidation does not result in such high $\delta^{18}O_{SO_4}$ values. However in field sites, the O_2 incorporation into SO_4^{2-} via direct reaction with pyrite–S sites may occur not only during initial oxidation but also during later stages of oxidation. It may be linked to the presence of ultrafine-grained pyrite (Tichomirowa and Junghans, 2009; Heidel et al., 2009) and/or to wet–dry-changes which have been shown to increase $\delta^{18}O_{SO_4}$ values (Taylor et al., 1984; Tichomirowa and Junghans, 2009).

Furthermore, the experiments indicated that a lot of O_2 may be consumed by incorporation into water during cathodic reduction whereas only a small amount of O_2 is incorporated into SO_4^{2-} via intermediate reaction products. The observed $\varepsilon_{SO_4-O_2}$ value may suggest that O_2 accepts electrons predominantly from pyrite and not from dissolved Fe^{2+}. The oxidation of adsorbed Fe^{2+} by O_2 may be catalyzed onto the pyrite surface; but the lack of ^{32}S enrichment in SO_4^{2-} compared to pyrite argues against a significant Fe^{3+} production. Hence, O_2 may be an important electron acceptor from pyrite without being incorporated into the produced SO_4^{2-}, i.e., without affecting $\delta^{18}O_{SO_4}$ values. Thus, the conclusion that low $\delta^{18}O_{SO_4}$ values indicating water as the O source show that Fe^{3+} is the dominating oxidant under acid pH conditions (according to reaction (2)) could be questioned. However, microorganisms are often present in field sites. They may accelerate the Fe^{2+} oxidation which provides Fe^{3+}. Hence, Fe^{3+} may be the dominating oxidant

even under acid pH conditions. Nevertheless, the data show that the dominance of Fe^{3+} or O_2 as electron acceptors is not reflected by $\delta^{18}O_{SO_4}$ values alone (as was interpreted by e.g., Butler, 2007; Seal et al., 2008); but further factors like pH, DO concentrations, Fe^{3+} concentrations, and the occurrence of microorganisms must be considered.

5. Conclusions

Abiotic pyrite oxidation experiments under aerobic acid conditions have been performed to investigate if (and how) O_2 is permanently incorporated into SO_4^{2-} during pyrite oxidation.

Increasing $\delta^{18}O_{SO_4}$ values with increasing injection volume of ^{18}O-enriched O_2 indicated that O_2 was permanently incorporated into the SO_4^{2-} produced during pyrite oxidation even after more than 151 days. The preferential consumption of ^{16}O during the pyrite oxidation experiments allowed the estimation of the O isotope enrichment factor $\varepsilon_{SO_4-O_2} = -8.4‰$ which was similar to that previously published $\varepsilon_{SO_4-O_2} = -9.8‰$ from Balci et al. (2007).

However, only $4.0 \pm 0.1\%$ (1σ, $n = 8$) of the consumed O_2 was incorporated into SO_4^{2-}. Hence, an additional mechanism has occurred where $96.0 \pm 0.1\%$ (1σ, $n = 8$) of the consumed O_2 was used. Slightly increased $\delta^{18}O_{H_2O}$ values in experiments with the largest injection volume of ^{18}O-enriched oxygen indicated that O_2 was consumed by incorporation into water molecules which may occur during the cathodic reduction of O_2. Hence, O_2 was an important electron acceptor under aerobic acid conditions. The observed $\varepsilon_{SO_4-O_2}$ value indicated that the oxidation of dissolved Fe^{2+} by O_2 did not play an important role. Furthermore, the lack of ^{32}S enrichment in SO_4^{2-} compared to pyrite indicated that the oxidation of adsorbed Fe^{2+} by O_2 should not be a dominant mechanism, although it may be catalyzed onto the pyrite surface. Hence, O_2 should accept electrons predominantly from pyrite. Ferric iron should play no important role as an electron acceptor during the pyrite oxidation experiments.

The incorporation of a small amount of the consumed O_2 into SO_4^{2-} resulted in a relative proportion of $9 \pm 3\%$ (1σ) O_2 (and, thus, $91 \pm 3\%$ (1σ) water-derived O) in SO_4^{2-} which is in the range of previous pyrite oxidation studies (e.g., Taylor et al., 1984; Reedy et al., 1991; Balci et al., 2007; Tichomirowa and Junghans, 2009; Heidel et al., 2009). Water-derived O may be incorporated into SO_4^{2-} via hydroxyl attack on pyrite–S sites promoted by nearby adsorbed O_2 on pyrite–Fe sites (according to Rosso et al., 1999; Rimstidt and Vaughan, 2003; Rosso and Vaughan, 2006). A direct reaction of O_2 with pyrite–S sites may only occur during the initial oxidation. The permanent incorporation of O_2 into SO_4^{2-} may occur by oxidation of the S intermediate species sulfite (and maybe tetrathionate) to SO_4^{2-}. However, some inconsistencies exist between the proposed mechanism and the obtained experimental data. Hence, future investigations of pyrite oxidation should include sulfite and tetrathionate oxidation experiments at acid pH conditions. The presence and concentrations of O_2, Fe^{3+}, and pyrite should be varied to obtain reaction rates, O isotope data, and O isotope enrichment factors for different conditions. However, experiments are difficult to perform due to the extremely fast kinetics of sulfite oxidation at acid pH.

Acknowledgements

We are grateful to R. Liebscher for supporting us with the sampling and for carrying out the isotope measurements. This study was funded by the German Research Foundation (DFG). We thank two anonymous reviewers, the Associate Editor Robert R. Seal and the Executive Editor Ron Fuge for their helpful comments which substantially improved the manuscript.

References

Balci, N., Shanks III, W.C., Mayer, B., Mandernack, K.W., 2007. Oxygen and sulfur isotope systematics of sulfate produced by bacterial and abiotic oxidation of pyrite. Geochim. Cosmochim. Acta 71, 3796–3811.

Basolo, F., Pearson, R.G., 1967. Mechanisms of Inorganic Reactions: A Study of Metal Complexes in Solution. Wiley, New York, USA.

Bonnissel-Gissinger, P., Alnot, M., Ehrhardt, J.-J., Behra, P., 1998. Surface oxidation of pyrite as a function of pH. Environ. Sci. Technol. 32, 2839–2845.

Brunner, B., Mielke, R.E., Coleman, M., 2006. Abiotic oxygen isotope equilibrium fractionation between sulfite and water. In: American Geophysical Union, Fall Meeting 2006, Abstract #V11C-0601.

Butler, T.W., 2007. Isotope geochemistry of drainage from an acid mine impaired watershed, Oakland, California. Appl. Geochem. 22, 1416–1426.

Ding, T., Valkiers, S., Kipphardt, H., De Bièvre, P., Taylor, P.D.P., Gonfiantini, R., Krouse, R., 2001. Calibrated sulfur isotope abundance ratios of three IAEA sulfur isotope reference materials and V-CDT with a reassessment of the atomic weight of sulfur. Geochim. Cosmochim. Acta 65, 2433–2437.

Druschel, G.K., Hamers, R.J., Banfield, J.F., 2003. Kinetics and mechanism of polythionate oxidation to sulfate at low pH by O_2 and Fe^{3+}. Geochim. Cosmochim. Acta 67, 4457–4469.

Epstein, S., Mayeda, T., 1953. Variation of O^{18} content of waters from natural sources. Geochim. Cosmochim. Acta 4, 213–224.

Giesemann, A., Jäger, H.-J., Norman, A.L., Krouse, H.R., Brand, W.A., 1994. On-line sulfur-isotope determination using an elemental analyzer coupled to a mass spectrometer. Anal. Chem. 66, 2816–2819.

Gleisner, M., Herbert Jr., R.B., Frogner Kockum, P.C., 2006. Pyrite oxidation by *Acidithiobacillus ferrooxidans* at various concentrations of dissolved oxygen. Chem. Geol. 225, 16–29.

Gould, W.D., McCready, R.G.L., Rajan, S., Krouse, H.R., 1989. Stable isotope composition of sulphate produced during bacterial oxidation of various metal sulphides. In: Salley, J., McCready, R.G.L., Wichlacz, P.L. (Eds.), Biohydrometallurgy. Proc. Internat. Symp. at Jackson Hole, Wyoming, August 13–18, 1989. The Minerals, Metals and Materials Society, Ottawa, Ontario, Canada, pp. 82–91.

Heidel, C., Tichomirowa, M., Junghans, M., 2009. The influence of pyrite grain size on the final oxygen isotope difference between sulphate and water in aerobic pyrite oxidation experiments. Isotopes Environ. Health Stud. 45, 321–342.

Holmes, P.R., Crundwell, F.K., 2000. The kinetics of the oxidation of pyrite by ferric ions and dissolved oxygen: an electrochemical study. Geochim. Cosmochim. Acta 64, 263–274.

Holt, B.D., Kumar, R., Cunningham, P.T., 1981. Oxygen-18 study of the aqueous-phase oxidation of sulfur dioxide. Atmos. Environ. 15, 557–566.

Hubbard, C.G., Black, S., Coleman, M.L., 2009. Aqueous geochemistry and oxygen isotope compositions of Acid Mine Drainage from the Río Tinto, SW Spain, highlight inconsistencies in current models. Chem. Geol. 265, 321–334.

Kamei, G., Ohmoto, H., 2000. The kinetics of reactions between pyrite and O_2-bearing water revealed from in situ monitoring of DO, Eh and pH in a closed system. Geochim. Cosmochim. Acta 64, 2585–2601.

Kornexl, B.E., Gehre, M., Höfling, R., Werner, R.A., 1999. On-line $\delta^{18}O$ measurement of organic and inorganic substances. Rapid Commun. Mass Spectrom. 13, 1685–1693.

Kroopnick, P., Craig, H., 1972. Atmospheric oxygen: isotopic composition and solubility fractionation. Science 175, 54–55.

Krouse, H.R., Gould, W.D., McCready, R.G.L., Rajan, S., 1991. ^{18}O incorporation into sulphate during the bacterial oxidation of sulphide minerals and the potential for oxygen isotope exchange between O_2, H_2O and oxidized sulphur intermediates. Earth Planet. Sci. Lett. 107, 90–94.

Lloyd, R.M., 1967. Oxygen-18 composition of oceanic sulfate. Science 156, 1228–1231.

Mazumdar, A., Goldberg, T., Strauss, H., 2008. Abiotic oxidation of pyrite by Fe(III) in acidic media and its implications for sulfur isotope measurements of lattice-bound sulfate in sediments. Chem. Geol. 253, 30–37.

Moses, C.O., Nordstrom, D.K., Herman, J.S., Mills, A.L., 1987. Aqueous pyrite oxidation by dissolved oxygen and by ferric iron. Geochim. Cosmochim. Acta 51, 1561–1571.

Nordstrom, D.K., 1982. Aqueous pyrite oxidation and the consequent formation of secondary iron minerals. In: Kittrick, J.A., Fanning, D.S., Hossner, L.R. (Eds.), Acid Sulfate Weathering, Special Publication No. 10. Soil Science Society of America, SSSA, Madison, Wisconsin, USA, pp. 37–56 (Chapter 3).

Nordstrom, D.K., Wright, W.G., Mast, M.A., Bove, D.J., Rye, R.O., 2007. Aqueous-sulfate stable isotopes – a study of mining-affected and undisturbed acidic drainage. In: Church, S.E., von Guerard, P., Finger, S.E. (Eds.), Integrated Investigations of Environmental Effects of Historical Mining in the Animas River Watershed, San Juan County, Colorado. US Geol. Surv. Prof. Paper 1651, pp. 391–416 (Chapter E8).

Oba, Y., Poulson, S.R., 2009a. Oxygen isotope fractionation of dissolved oxygen during abiological reduction by aqueous sulfide. Chem. Geol. 268, 226–232.

Oba, Y., Poulson, S.R., 2009b. Oxygen isotope fractionation of dissolved oxygen during reduction by ferrous iron. Geochim. Cosmochim. Acta 73, 13–24.

Pisapia, C., Chaussidon, M., Mustin, C., Humbert, B., 2007. O and S isotopic composition of dissolved and attached oxidation products of pyrite by *Acidithiobacillus ferrooxidans*: comparison with abiotic oxidations. Geochim. Cosmochim. Acta 71, 2474–2490.

Reedy, B.J., Beattie, J.K., Lowson, R.T., 1991. A vibrational spectroscopic ^{18}O tracer study of pyrite oxidation. Geochim. Cosmochim. Acta 55, 1609–1614.

Rimstidt, J.D., Vaughan, D.J., 2003. Pyrite oxidation: a state-of-the-art assessment of the reaction mechanism. Geochim. Cosmochim. Acta 67, 873–880.

Rosso, K.M., Vaughan, D.J., 2006. Reactivity of sulfide mineral surfaces. In: Vaughan, D.J. (Ed.), Sulfide Mineralogy and Geochemistry. Reviews in Mineralogy, vol. 61, pp. 557–607 (Chapter 10).

Rosso, K.M., Becker, U., Hochella Jr., M.F., 1999. The interaction of pyrite {1 0 0} surfaces with O_2 and H_2O: fundamental oxidation mechanisms. Am. Mineral. 84, 1549–1561.

Seal II, R.R., 2003. Stable-isotope geochemistry of mine waters and related solids. In: Jambor, J.L., Blowes, D.W., Ritchie, A.I.M. (Eds.), Environmental Aspects of Mine Wastes, Mineralogical Association of Canada, Short Course Series, vol. 31. Vancouver, British Columbia, Canada, pp. 303–334 (Chapter 15).

Seal II, R.R., Hammarstrom, J.M., Johnson, A.N., Piatak, N.M., Wandless, G.A., 2008. Environmental geochemistry of a Kuroko-type massive sulfide deposit at the abandoned Valzinco mine, Virginia, USA. Appl. Geochem. 23, 320–342.

Singer, P.C., Stumm, W., 1970. Acidic mine drainage: the rate-determining step. Science 167, 1121–1123.

Taylor, B.E., Wheeler, M.C., 1994. Sulfur- and oxygen-isotope geochemistry of Acid Mine Drainage in the Western United States. In: Alpers, C.W., Blowes, D.W. (Eds.), Environmental Geochemistry of Sulfide Oxidation. Am. Chem. Soc. Symp. Series 550, pp. 481–514 (Chapter 30).

Taylor, B.E., Wheeler, M.C., Nordstrom, D.K., 1984. Stable isotope geochemistry of Acid Mine Drainage: experimental oxidation of pyrite. Geochim. Cosmochim. Acta 48, 2669–2678.

Thurston, R.S., Mandernack, K.W., Shanks III, W.C., 2010. Laboratory chalcopyrite oxidation by *Acidithiobacillus ferrooxidans*: oxygen and sulfur isotope fractionation. Chem. Geol. 269, 252–261.

Tichomirowa, M., Junghans, M., 2009. Oxygen isotope evidence for sorption of molecular oxygen to pyrite surface sites and incorporation into sulfate in oxidation experiments. Appl. Geochem. 24, 2072–2092.

Toran, L., 1986. Sulfate contamination in groundwater near an abandoned mine: hydrochemical modelling, microbiology and isotope geochemistry. PhD thesis. Univ. Wisconsin-Madison.

Wassenaar, L.I., Koehler, G., 1999. An on-line technique for the determination of the $\delta^{18}O$ and $\delta^{17}O$ of gaseous and dissolved oxygen. Anal. Chem. 71, 4965–4968.

Williamson, M.A., Rimstidt, J.D., 1994. The kinetics and electrochemical rate-determining step of aqueous pyrite oxidation. Geochim. Cosmochim. Acta 58, 5443–5454.